45TH TURBOMACHINERY & 32ND PUMP SYMPOSIA
HOUSTON, TEXAS | SEPTEMBER 12 – 15, 2016
GEORGE R. BROWN CONVENTION CENTER

THE APPLICATION OF ULTRASONIC TECHNOLOGY TO IMPROVE THE RELIABILITY OF MAGNETIC-DRIVE CENTRIFUGAL PUMPS

Samuel Tomlinson
Product Development Engineer
Sundyne HMD Kontro Sealless Pumps Ltd.
Eastbourne, East Sussex, UK

David Clark
Senior Engineering Manager
Sundyne HMD Kontro Sealless Pumps Ltd.
Eastbourne, East Sussex, UK

Andrew Hunter
Head of Research and Development
Tribosonics Ltd.
Sheffield, South Yorkshire, UK

Samuel Tomlinson is a Product Development Engineer at Sundyne HMD Kontro Sealless Pumps Ltd, Eastbourne, England. He has 3 years of experience, primarily focussing on the incorporation of ultrasonic technology into HMD magnetic-drive pumps, although he also has experience in pump applications. Samuel graduated as a Master of Engineering in the field of Mechanical Engineering from the University of Surrey (United Kingdom) in 2013 and is currently working towards his Chartership with the Institution of Mechanical Engineers (IMechE).

David Clark is the Senior Engineering Manager of Sundyne HMD Sealless Pumps Ltd, Eastbourne, England. He has been with the organisation for over 30 years and took responsibility for the Engineering and Product Development groups in 1998. David is a Chartered Engineer with the Institution of Mechanical Engineers (IMechE) and is a serving member on API Sub Committees on Machinery Equipment including API 685 and ASME B73.3. He has implemented numerous sealless products and services including high system pressure pump ranges, API vertical pump ranges, a high efficiency engineered composite containment shell, and an ultrasonic condition monitoring device.

Andrew Hunter is the Head of Research & Development at Tribosonics Ltd. having joined the company in 2009. He works across a range of sectors providing services and developing products to measure aeration, stress, wear, corrosion, real area of contact and thin embedded films using ultrasonic techniques. He graduated as a Master of Engineering in the field of Mechanical Engineering from the University of Sheffield (United Kingdom), where he is now writing up a PhD thesis on the ultrasonic monitoring of cold metal rolling.

ABSTRACT

It is widely acknowledged that sealless magnetic drive pumps give total containment of the pumped process liquid, which in an industry where there are ever tightening environmental constraints on plant operation and increasing health and safety requirements, offers a real advantage of reliability and safety to users.

However, as with any piece of process machinery, magnetic drive pumps are designed to operate within specific parameters and operation outside of these parameters can lead to reduced levels of reliability. Whilst traditional instrumentation (measurement of temperature or power) will assist in improving the reliability of the machine, these instruments are not monitoring the primary cause of the issue; instead they are monitoring the effect that the fault condition has on another part of the machine.

By constantly monitoring the condition of the pumped liquid present in the internal flow regime of a magnetic-drive pump, it is

possible to rapidly identify potential issues and react to them accordingly. Ultrasonic technology has been utilised to rapidly and accurately detect the presence of vapour in the liquid stream. The technology provides a precise and sensitive response to even the smallest change in phase, therefore improving the overall reliability of the machine.

This paper presents an overview of the ultrasonic technology that has been utilised to monitor the condition of magnetic-drive centrifugal pumps, including highlights of extensive testing that has been carried out and some real world examples involving the application of this technology on volatile light hydrocarbon processes.

INTRODUCTION

A magnetic-drive, sealless, centrifugal pump offers complete containment of process liquid, utilizing product lubricated bearings within a pressure boundary and a magnetic coupling to transmit torque across a containment shell. A cross-section of a typical magnetic-drive centrifugal pump is shown in Figure 1.

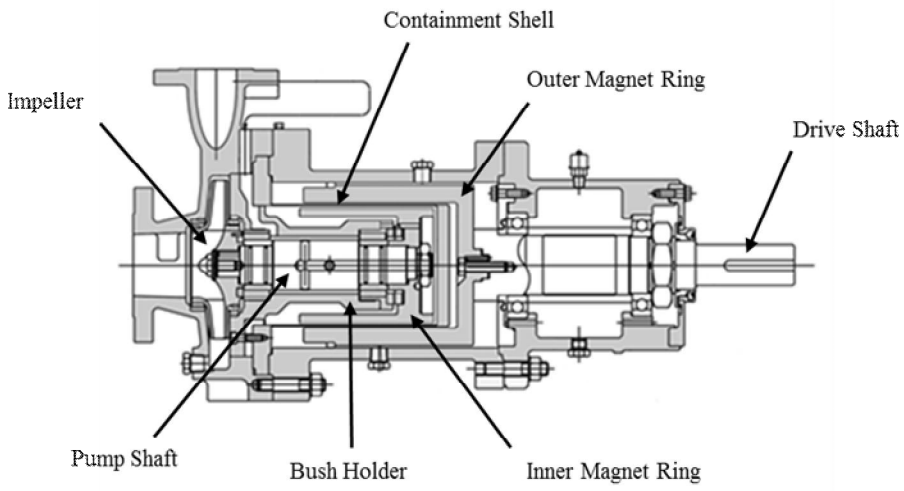

Figure 1: Cross-Section of a Typical API 685 Magnetic Drive Centrifugal Pump.

A pump casing consists of the suction and discharge flanges and the casing volute which houses the impeller. Rotation of the impeller imparts energy to the liquid causing the pump to operate. The impeller is supported by the internal pump shaft and shaft sleeves. The shaft is supported by the bush holder consisting of a rigid holder and bushes or bearings which run against the shaft sleeves. Completing the inner rotor assembly is the inner magnetic ring. This is a ring of co-axially arranged outward facing permanent magnets, which are fully encapsulated with a resistant metallic sheathing. The final component of the liquid contact assembly is the containment shell. This component is statically sealed with a gasket against the casing. The containment shell is usually manufactured from a high strength, non-magnetic, corrosion resistant alloy. Outside of the primary pressure boundary is a second, outer magnetic ring, with magnets that face inwards. The outer magnetic ring is located in the coupling housing which is connected to the external bearing assembly. When the pump is filled or ‘primed’, the liquid is completely contained without the use of any dynamic seals. The principle of operation is very simple. The magnets in the outer and inner magnet rings are attracted to each other, so as the electric motor rotates, the outer ring and the inner ring rotate at the same speed, thus rotating the impeller and causing liquid to be pumped.

The containment shell is located between the two attracting magnetic rings, and will be subjected to the rotating magnetic circuits as the outer and inner magnetic rings rotate. For strength and temperature resistance, the containment shell is usually manufactured in a metallic material which is electrically conductive. It is this property in conjunction with the rotating magnetic circuits that causes eddy currents to be induced in the containment shell. These induction losses manifest themselves as heat and have to be accounted for when applying the pump.

A small portion of the pumped liquid is also used to cool the magnetic coupling and lubricate the internal bearings. The pump uses the

pressure generated by the impeller to feed a small amount of pumped product into the rear of the pump. Here the flow splits and a small portion of the flow lubricates the internal plain bearings and returns to the pump casing volute. The majority of the flow enters the holes in the pump shaft and travels to the rear of the containment shell where it splits radially and flows along the annulus between inner magnetic ring and the containment shell tube. As already mentioned the metallic containment shell has associated losses, which need to be cooled, and it is this internal flow that provides this cooling. After the flow has travelled over the inner magnetic ring, it then returns to the bulk flow in the casing volute through the return feed hole behind the rear of the impeller.

It is important to understand the impact of circulating the pumped liquid in the internal feed system. As the liquid is circulated, its pressure drops and temperature increases, and for safe and reliable operation, the liquid needs to remain stable at all times.

It has often been suggested that monitoring the condition of the internal flow would be of great assistance to the user of magnetic drive pumps, in particular with regards to vapour content. However, the technicality of implementing such a system has proven to be particularly challenging. The pump construction prevents easy access to the process liquid that is circulated in the rear of the pump, as the pressure boundary (containment shell), is surrounded by the rotating outer magnet ring. Furthermore, if this boundary was breached to gain access to the liquid, it would effectively lose its Sealless characteristic, thus non-invasive techniques would be preferred.

THE EFFECT OF VAPOUR ON THE RELIABILITY OF MAGNETIC-DRIVE CENTRIFUGAL PUMPS

There are a few failure mechanisms that exist for magnetic-drive centrifugal pumps; these include vapourisation of the pumped product, the presence of gas in the process stream, operation with a lack of prime, off-curve operation and running with a closed valve. This section provides an overview of some of these failure modes.

The majority of magnetic-drive pumps utilise Silicon Carbide (SiC) for the internal, process lubricated bearings. It is widely acknowledged that when wet, this material is superior to the historically used carbon bearings; this is due to the extremely low coefficient of friction, which means that it will not wear when adequately lubricated. Therefore when a magnetic-drive pump is applied correctly, maintenance will not be required to change bearings, subsequently decreasing the pump downtime and reducing cost. However when SiC is used as a bearing material in a dry, non-lubricated environment, the coefficient of friction is extremely high. This property, in conjunction with the poor heat propagation through the material, means that when the SiC-on-SiC bearings are not lubricated and the pump is operated, the contacting surface of the material increases in temperature extremely quickly whilst the remaining material will remain ‘cool’. The difference in the coefficient of expansion (due to temperature difference) between the front, contacting face and the rear face can be large and therefore micro-cracks may propagate on the heated face under this upset condition. SiC is available in different compositions and/or with various coatings (for example diamond-like coatings) which can reduce the friction coefficient and aid in the tolerance of the material to upset, dry-running conditions. However it should be noted that these do not address the root cause of the issue.

The API 685 standard (2011) requires the vendor to provide calculations for the variation in product pressure against temperature as the liquid is circulated through the rear of the pump. This is compared to the variation in liquid vapour pressure with temperature, to ensure that the product remains in liquid state. A typical example of a pressure-temperature calculation can be seen in Figure 2.

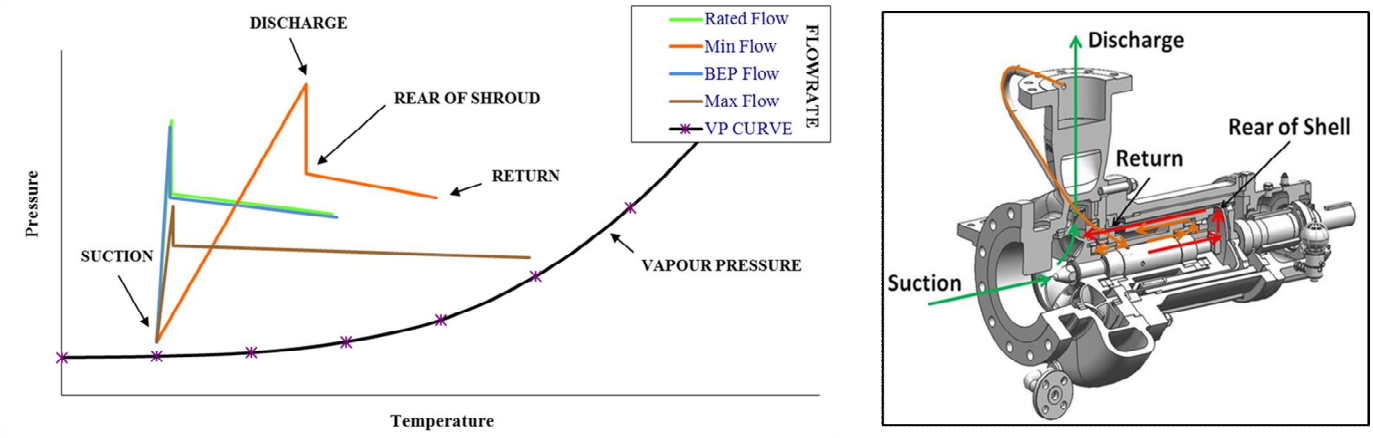

Figure 2: Pressure-Temperature Calculation for an Aromatic Hydrocarbon Application.

As can be seen in the example of the pressure-temperature calculation above, the internal flow gradually reduces in pressure as it follows the path through the rear of the pump. In addition, there are several sources of heating, the most significant of which is eddy current heating when a metallic containment shell is employed within a pump. The most significant consequence of eddy current heating is the possible vapourisation of the liquid in the rear of the pump. Certain liquids are more susceptible to this vapourisation; particularly liquids with high vapour pressure characteristics, which require higher pressures to remain in liquid state, and low specific heat liquids, which require less additional energy to experience a temperature rise. As indicated previously, the impact of eddy current heating needs to be carefully considered when applying magnetic-drive centrifugal pumps.

As mentioned previously, the presence of gas in the process stream can be problematic for magnetic-drive centrifugal pump performance. The head drop caused by gas entrainment has potential to reduce the internal flow, consequently reducing the lubrication and cooling of the pump internals. If the liquid film between the bearings is reduced, they can become damaged (as previously explained), and the reduction in cooling of the magnetic coupling can further promote product vapourisation in the rear of the pump. Large ‘slugs’ of gas will fill the entire pump, preventing liquid discharge. This volume of liquid contained within the pump will recirculate through the internal flow regime and is exposed to eddy current heating. This again presents the possibility of product vapourisation and damage to the pump internals.

Another potential failure mechanism of magnetic-drive centrifugal pumps is operation with a lack of prime. If the pump is started without being adequately primed, the internal bearings will not be lubricated which might lead to premature failure. This may happen after routine pump service. Operation malpractice can also present as a failure mechanism. For instance, operation with a reduced flow rate, caused by a partially closed suction valve or discharge valve, may take the duty point to below the minimum safe flow threshold. This can induce cavitation which can lead to the failure of the pump. Operation with a completely closed suction valve can be extremely destructive. In this condition, the process liquid will not discharge from the pump and is instead exposed to continuous eddy current heating as the fixed volume of liquid is circulated through the internal pump channels. Cooling from a fresh feed does not occur and therefore the liquid and pump internals will experience a rapid rise in temperature. This too may cause product vapourisation.

Many of these failures could be avoided by monitoring the vapour content in the rear of the pump. This would give the operator a clear indication preventing dry-starts, and a way of monitoring vapour generated through incorrect pump operation or changing process conditions. By feeding vapour content information into the pump control system, the pump could be shut-down before damage occurs.

OVERVIEW OF METHODS FOR DETECTION OF GAS IN LIQUID

There have been a number of studies researching the detection of gas in liquids. Non-invasive methods used in these studies have included electrical impedance, radiography, optical and acoustic (Xu and Chahine, 2010).

Tomographic electrical impedance methods have been shown to be capable of measuring gas and particle distributions in a two-phase liquid flow (George et al, 2000). This method builds up a two-dimensional picture of the flow by using multiple sensors. The method could be used with a sensor pair, however to apply this to a sealless pump this would require the placement of sensor inside the containment shell, and wiring to this. It also needs the components on both sides of the flow to be electrically isolated, making it unsuitable to be retrofitted to existing pumps. Radiography techniques, while effective, involve expensive and bulky equipment making them unsuitable for widespread industrial use (Riemer et al, 1997).

Optical methods have several advantages. Firstly detectors used in this method are phase insensitive, light that has been scattered by the presence of bubbles and is received as a combination of signals is often still detectable (Povey, 1997). This makes light methods suitable where there is a large gas content. Optical methods are hindered by opaque liquids and materials. Applications like magnetic drive pumps which have metallic or similarly opaque containing materials would require either the detection device to be invasive to the process liquid, or the insertion of a transparent window, both of which would penetrate the containment boundary making this approach unsuitable. Instead a method needs to found which is non-invasive to the containment boundary or process liquid.

It has been well documented that gas bubbles have a significant effect on the propagation of ultrasound. Conversely this sensitivity has meant that acoustic approaches have found a use as a gas detection method in applications which vary from the detection of bubbles in medical intravenous lines, to the characterisation of aerated foodstuffs (Mason & Povey, 1997). With ultrasonic methods it is possible to mount the sensor on the external surface of a part, without the need for invasive probes or windows as required by optical techniques. This means that there would be no need to penetrate the containment boundary. Also unlike optical methods, acoustic waves suffer from interference caused by scattered signals of different phases; this can be used as a method for gas detection. It has therefore been proposed that an ultrasonic detection method could be applied to magnetic-drive sealless pumps to detect vapour content in the rear of the pump and prevent the failure mechanisms that are induced.

ULTRASONIC THEORY

Ultrasound is any acoustic signal with a frequency above the range of human hearing (~20 kHz). It is widely employed in Non-Destructive Testing (NDT) and thickness gauging where the frequency range normally used is approximately 100 kHz to 50 MHz. The following section outlines some of the basic ultrasonic theory used in this paper.

Propagation and Speed of Sound

Ultrasonic waves are simply pressure waves made of successive compressions and rarefactions. Unlike Electromagnetic (EM) waves, they require an elastic medium such as a liquid or a solid to propagate. While a number of wave modes exist, this paper will only deal with longitudinal waves, which are compressional waves where the particle motion is in the same direction as the propagation of the wave. The speed of wave propagation is an important parameter and is related to the wavelength and frequency according to the following relationship shown in Equation (1):

$$c = \lambda f \tag{1}$$

Where **c** is the speed of sound, **λ** is the wavelength and **f** is the frequency. The speed of sound within a material is defined predominantly by its density and elasticity. Elastic properties relate to the tendency of a material to maintain its shape and not deform when a force is applied to it. At the particle level, a rigid material is characterized by atoms and/or molecules with strong forces of attraction for each other. These forces can be thought of as springs that control how quickly the particles return to their original positions. Particles that return to their resting position quickly are ready to move again more quickly, and thus they can vibrate at higher speeds. Therefore, sound can travel faster through a medium with higher elastic properties, like steel, than it can through a medium like rubber, which has lower elastic properties.

A substance that is denser per unit volume has more mass per volume, with larger molecules typically having more mass. If a material

is denser because of larger molecules, it will transmit sound slower. This is because sound waves are made up of kinetic energy. It takes more energy to make large molecules vibrate than it does to make smaller molecules vibrate. Sound will therefore travel at a slower rate in the denser object with the same elastic properties. This is counterintuitive; it is commonly thought that sound travels faster in solids than liquids and gases due to their higher density, in fact it is due to the solid's higher stiffness. The speed of sound in a liquid can be calculated from its density and compressibility, using the relationship shown in Equation (2).

$$c = \sqrt{\frac{1}{\beta_a \rho}} \qquad 2$$

Where β_a is the adiabatic compressibility and ρ is the density. Table 1 presents the speed of sound for some common materials and also provides the 10MHz wavelength which was calculated using Equation (1).

Table 1: Typical Speed of Sound and Wavelength of Common Materials, Reproduced from National Physics Laboratory (n.d.).

	Speed of Sound **c,** m/s	**Wavelength (@10MHz)** **λ,** μm	**Attenuation Coefficient (@10MHz)** **α,** Nepers/m	**Acoustic Impedance** **Z,** MRayls
Air (20°C, 10% Relative Humidity)	344	34	-	0.004
Methanol	1103	110	3.2	0.889
Distilled Water (20°C)	1482	148	2.5	1.483
Glycerol	1920	192	~300	2.42
Hardened Tool Steel	5874	587	4.94	46

It is important to understand the speed of sound within a material for a number of reasons. By recording how long it takes an ultrasonic wave to propagate through a material, and knowing the speed of sound in the material, the thickness of the material can be calculated. If a short ultrasonic impulse is generated into an object, any waves received can be displayed as function of time and therefore depth. This is the basis behind ultrasonic thickness gauging. Where the intention is to study a wave from a particular source, the speed of sound is required to identify in time which wave to study. As the speed of sound will vary with temperature within a material, the wave position will shift according to the temperature, and this must be taken into account when processing the signals. Where measurements are taken at high speed it is necessary to allow enough time for the wave of interest to return before the next ultrasonic impulse is generated, again this is a function of the distance and speed of sound.

Attenuation and Scattering

Sound does not propagate through a material without losses. Causes of losses include scattering, diffusion, viscous damping losses and relaxation losses. These losses can be grouped into three categories, collectively known as the material's *Attenuation*. *Scattering* is the reflection of sound waves from inclusions or rough grain structure, such as that found in cast iron or an aerated liquid. This causes the waves to deflect away from the receiving sensor resulting in a reduction in the received signal. *Absorption* is the inefficiency of a material in transmitting a sound wave. As a wave propagates through a material, part of its energy is converted to heat; rubbers and plastics are examples of highly absorbing materials. *Geometric Attenuation* occurs where wave propagation is altered away from the receiving transducer due to the shape of the material. It is worth noting that a wave will also decrease in intensity with distance due to the spread of the ultrasonic beam. The attenuation of a material is characterised by its attenuation coefficient, as shown in Equation (3).

$$\frac{I_2}{I_1} = e^{-2\alpha} \qquad 3$$

Where I_1 and I_2 are the intensity of a wave before and after it has propagated a unit distance through a material respectively, and α is the attenuation coefficient, normally quoted in Nepers/m (although this can be converted to dB/m by multiplying by a factor of 8.686). Table 1 gives typical values for attenuation coefficients. To ensure that a returned wave is measureable and is not overly attenuated, it is necessary to ensure that the incident wave has sufficient intensity. As with the speed of sound, the attenuation in a material changes

with temperature. If this is not accounted for, it will manifest itself as an error in any wave amplitude measurements taken.

Soundwave Behaviour at Interfaces

A useful value for characterising the acoustic behaviour of a material is its acoustic impedance, which is the product of the materials density and speed of sound as shown in Equation (4).

$$Z = \rho c \tag{4}$$

Where **Z** is the acoustic impedance. Measured in Rayls, solids typically have high acoustic impedances in the 10's of MRayls, liquids are approximately 0.8 to 2 MRayls (Xactec Corporation, n.d.) and gases have a much lower acoustic impedance due to their low density and low speed of sound (Alter, et al., 2012). Typical acoustic impedances are given in Table 1. When a sound wave reaches the interface between two media of differing acoustic impedances, then only part of the wave will transmit across the boundary, and part will reflect. The amplitude of the reflected wave can be calculated using Equation (5).

$$A_R = A_I\left(\frac{Z_2 - Z_1}{Z_1 + Z_2}\right) \tag{5}$$

Where $\mathbf{A_I}$ and $\mathbf{A_R}$ are the amplitudes of the incident and reflected waves respectively and $\mathbf{Z_1}$ and $\mathbf{Z_2}$ are the acoustic impedances of the materials either side of the interface. Equation (5) is often simplified to give a reflection coefficient **R** which is the ratio of the reflected and incident amplitudes ($\mathbf{A_R/A_I}$). The amplitude of the transmitted wave, defined by the transmission coefficient **T**, is simply calculated by T=R+1. Table 2 gives the reflection and transmission coefficients for some example interfaces as calculated using Equation (5), values for acoustic impedance are taken from Table 1.

Table 2: Example Interface Reflection and Transmission Coefficients.

	Reflection Coefficient, R	Transmission Coefficient, T
Steel to Air	-0.9998	0.0002
Steel to Water	-0.9375	0.0625
Water to Air	-0.9946	0.0054
Water to Steel	0.9375	1.9375

There are two points on interest in Table 2. Firstly, reflection coefficients for interfaces where the acoustic impedance is higher in the first material than the second are negative; this means the reflected wave is inverted. Secondly, the transmission coefficient for water to steel is greater than one. At first this may seem to contravene the conservation of energy law. However the amplitudes described here represent the sound pressure, not the energy, which is calculated from both the sound pressure and material acoustic impedance.

When a sound wave passes through a multi-layered system, reflections of varying amplitudes will be received from the interfaces between the materials. The amplitudes of these reflections is dependent upon the materials either side of the interface, and the attenuation through the materials.

UTILISING ULTRASONIC TECHNOLOGY TO DETECT GAS BUBBLES

Simplistically, gas bubbles can be thought of in the same manner as solid or liquid particles, with a few key differences. The large acoustic impedance difference results in almost total reflection from the liquid/gas interface. Bubbles can also exhibit resonant behaviour when subject to excitation; the surface energy of the bubble plays a significant role, meaning that more than one mode of resonance may be important.

Bubble Resonance

The first study of note into bubble acoustics was completed by Marcel Minnaert (1933). This defined the Minnaert Frequency; the frequency of resonance of a bubble. This resonance is the result of the balance between internal bubble pressure and force from the surrounding displaced liquid. Minnaert's calculations assume a single bubble with only one mode of resonance, however subsequent studies have since extended this work (Gaunaurd and Überall, 1981).

Bubble resonance offers a way of identifying and quantifying bubbles within a liquid. It is a passive approach achieved by simply listening for the energy released by events such as bubble formation or collapse. In many ways it is akin to the acoustic emissions measurements taken in the fields of structural integrity and rotating equipment monitoring. The acoustic output of the system is recorded and analysed for certain signature frequencies and events which signify failure modes. This approach requires a good understanding of the complete system under inspection and a profiling of the various conditions for each system setup (each different material and failure mode). It is also susceptible from extraneous environmental noise. The large degree of setup and tuning, along with the need to adequately remove external sources of noise, means that while this approach has value in research and high value applications, it is less viable for industrial monitoring of assets over which there is less control. Furthermore, the failure signatures are not well understood and the cost of a trained installer would be prohibitive.

A more robust approach is the use of active acoustics. This involves the generation of high-frequency sound waves which pass through the inspected medium and are captured and evaluated. Any change in the signal is the result of the material through which it has passed. Additionally, the properties of the induced wave can be selected to ensure their sensitivity only to the effects being studied. There are three common measurement types taken using this approach, these are *Time-of-Flight* (ToF), *Amplitude and Frequency* (Yim and Leighton, 2010). The approach adopted by Minnaert demonstrates an example of a frequency based method for bubble sizing, albeit a passive approach. Applications of the other two approaches are described below.

Time of Flight (ToF)

ToF works by relating the transit time of an ultrasonic pulse to the distance travelled via the speed of sound in the medium. This makes it a useful tool for distance measurement, or inversely the speed of sound measurement. Where bubble size is small comparative to the acoustic wavelength, a wave is able to propagate through the medium (as the attenuation is not too high), and if the liquid and gases are well understood, it is possible to relate the volume of each component in a gas/liquid mixture through the speed of sound. Figure 3 shows how the speed of sound relates to the volume fraction of air in water. Interestingly this plot demonstrates counter-intuitively that the speed of sound of a mixture is not the mean of the constituent parts, as for certain volume fractions the speed of sound for the mixture drops significantly below that for either air or water.

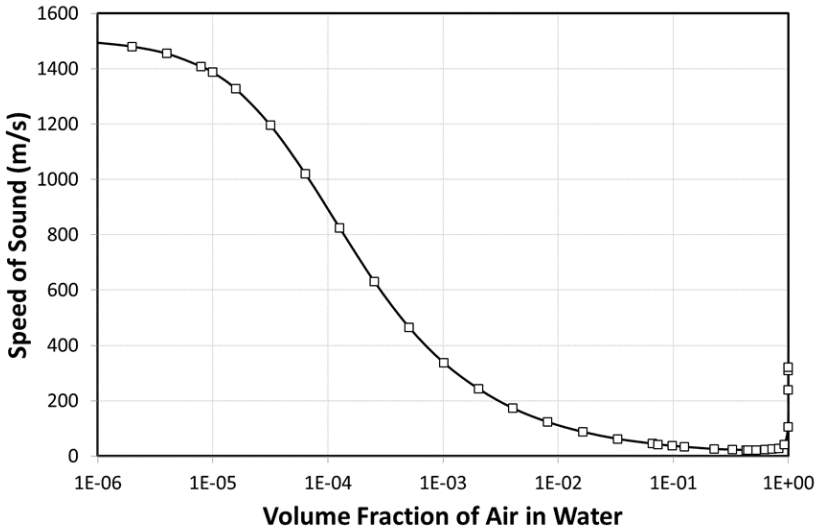

Figure 3: The Velocity of Sound in Air/Water Mixtures at 20°C (68°F), Reproduced from Povey (1997).

This method is limited in its use due to the low frequency and high amplitude incident wave required to overcome the high attenuation. It also assumes bubble sizes smaller than the wavelength used.

Amplitude

The size of a detectable defect is relative to the signal wavelength. Wavelength is related to wave frequency and speed of sound as defined in Equation (1), with example wavelengths given in Table 1. There is very poor transmission of sound from a liquid to a gas,

as exemplified earlier, transmission and attenuation into the bubble can therefore normally be ignored where the bubble is greater or comparable to the wavelength of the ultrasound within the process liquid. In this circumstance bubbles can be thought of as only scattering rather than absorbing the ultrasound.

Ozeri et al. (2006) demonstrated an amplitude based method which compared the magnitude of the transmitted and the received ultrasonic signals to detect the presence of bubbles in intravenous lines (using the test arrangement shown in Figure 4).

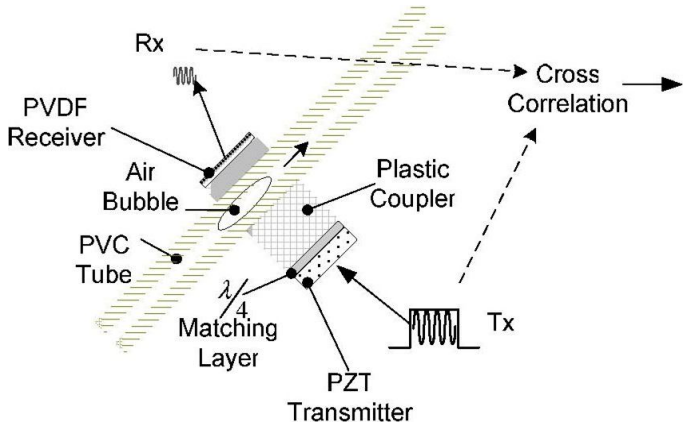

Figure 4: Example Test Arrangement for Amplitude Ultrasonic Detection, Courtesy of Ozeri, et al. (2006).

Due to the high reflection coefficient of the water-air interface most of the sound wave reaching an air bubble will be reflected, therefore not reaching the receiver. The amplitude of the transmitted wave is compared with the amplitude of the wave captured at the receiver, with any drop in amplitude a result of the cross-sectional area blocked by any intermediate air bubbles.

It is a similar cross-sectional area blocking technique that is used in this paper. This technique was selected as it offers a robust measurement. During normal operation (where no vapour is present) an ultrasonic signal is received; it is only in upset conditions (where vapour is present) that the signal will reduce or no signal be received. This also means any other failures in the system or measurement equipment which prevent a signal being received will result in the reporting of upset conditions, greatly reducing the chance of a false-positive reading.

A disadvantage of this technique is that it is only capable of giving a qualitative indication, rather than an accurate quantitative measurement of the vapour; it is incapable of ascertaining the actual volume of vapour, however testing has shown that this technique can provide a strong indication of quantity, providing that the system parameters and liquid characteristics are known. Despite this, the response of the system to fault conditions in the pump can be characterised for future reference.

APPLICATION SPECIFIC ULTRASONIC CONSIDERATIONS

There are a number of application specific features that must be considered when applying ultrasonic technology to magnetic-drive centrifugal pumps. These are outlined in this section.

Measurement Configuration
Being able to install the sensor in a manner that does not breach the primary pressure boundary of the magnetic-drive pump is highly desirable. This requires the sensor to be mounted on the external of the pressure containment shell. Fortunately the ultrasonic approach allows this; the sensor transmits the ultrasonic signal through the containment shell wall and the process liquid, where it reflects from the shoulder of the bush holder and returns to the sensor Figure 5.

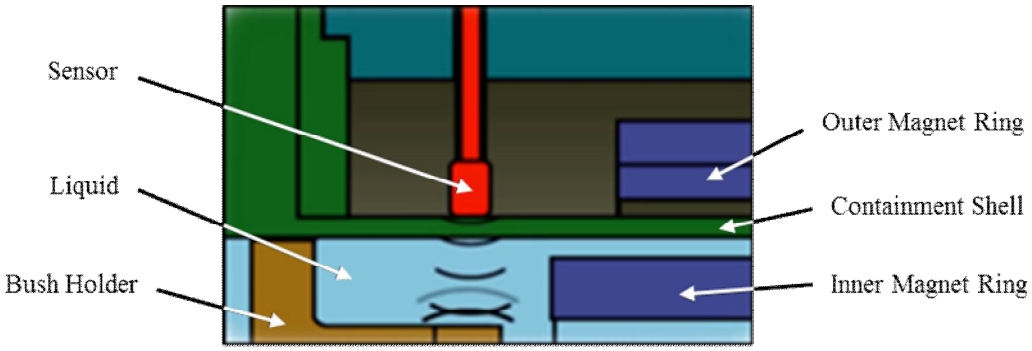

Figure 5: Ultrasonic Signal Path through a Magnetic-Drive Pump during Fully Primed, 100 Percent Liquid Condition.

This setup can be approximated to a steel-water-steel system, as shown in Figure 6. The figure shows three cases. The first is where there is air on the near steel face. This not only occurs because of the presence of bubbles, it is also commonly seen where a pump has been left standing, allowing absorbed gases to nucleate on surface. The second case shows reflections from a gas within a liquid, and the final case is with no gas.

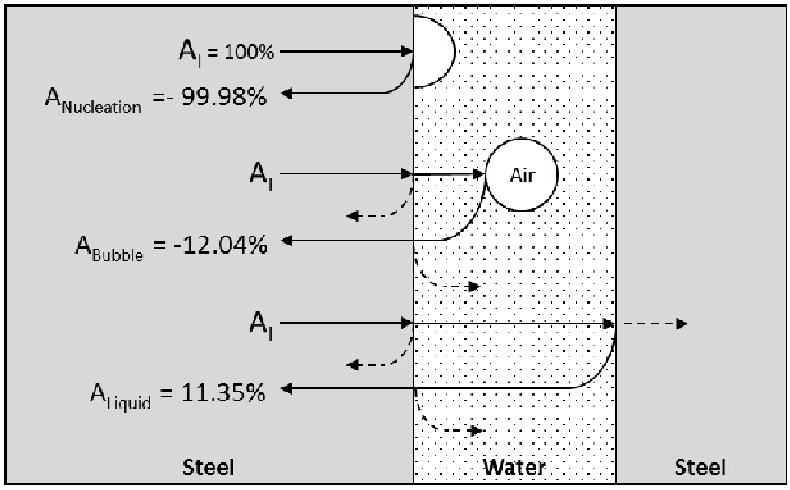

Figure 6: Ultrasonic Paths and Resultant Signal Amplitudes for Three Aeration Cases in a Steel-Water-Steel Arrangement.

By taking typical values for the acoustic impedance, and using Equation (5), it is possible to approximate the amplitude of the signal returned from the three cases shown. This approximation is simplistic, not taking into account the attenuation in the materials and beam spread. It also assumes the reflecting and bubble faces are flat and parallel, thereby ignoring any scattering effects. Nevertheless it can be seen that there is relatively little difference in the amplitude due to the acoustic impedance mismatch alone, except in the case where gas has formed on the near steel surface. What can also be noted from Figure 6 is the differing path lengths in each case, each of which will have a different ToF. It is therefore possible to discriminate in the time-domain between the waves reflected or scattered by bubbles, and the wave reflected from the far steel face. Figure 7 presents a pictorial representation of the aforementioned effects.

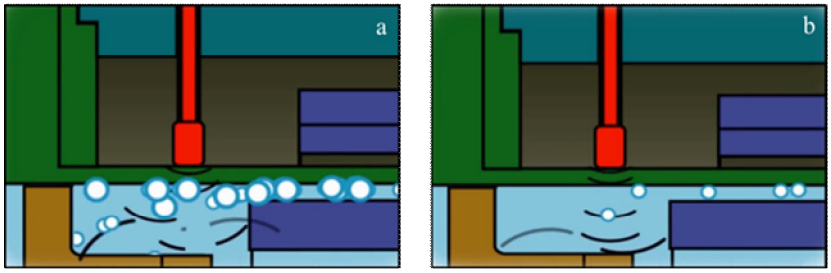

Figure 7: The Effect of a) Large Bubbles/Vapour Pockets and b) a Small Quantity of Vapour on the Ultrasonic Wave.

When the pump has a lack of prime (100 percent vapour condition), the ultrasonic signal does not transmit through the inner wall of the containment shell, in the same manner as the nucleation case shown earlier. Therefore, when the ultrasonic signal encounters the solid-vapour boundary, the signal does not transmit through the interface and is instead reflected back to the sensor from the inside wall of the containment shell (Figure 8).

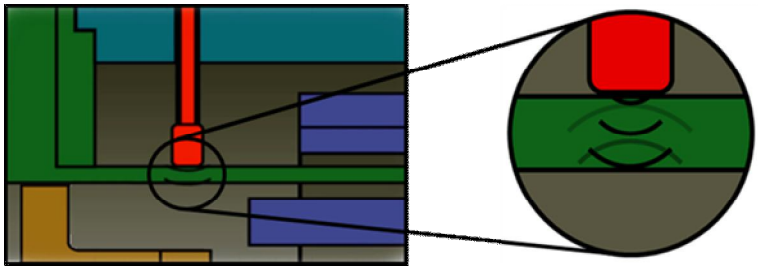

Figure 8: Ultrasonic Signal Path through a Magnetic-Drive Pump during Lack of Prime, 100 Percent Vapour Condition.

Material Considerations

Magnetic-drive pumps are used on a wide variety of process liquids seen in the chemical, petrochemical and oil and gas and sectors. Processes may be run at a different temperature, different applications will require different materials of construction of different dimensions, and the length of the liquid path through which the ultrasound is transmitted will also vary. The large number of variables makes the design of a system that is suitable for all applications almost impossible. Instead, to accommodate the varying signal attenuation and ToF, a small amount of calibration is required. This calibration is normally limited to adjusting the amplification required to counteract the attenuation, and the time at which the receiving hardware looks for a returned reflection. More details on the ultrasonic hardware are given in the following section.

ULTRASONIC INSTRUMENTATION

A number of elements make up an ultrasonic measurement system; an example of the key elements in a typical pulse-echo system can be seen in Figure 9. Selection of these components must not only be informed by measurement performance, but also application specific requirements including legislative, environmental, product lifetime, integration and security. These additional requirements are just as important for ensuring the measurement technique is viable in the proposed application.

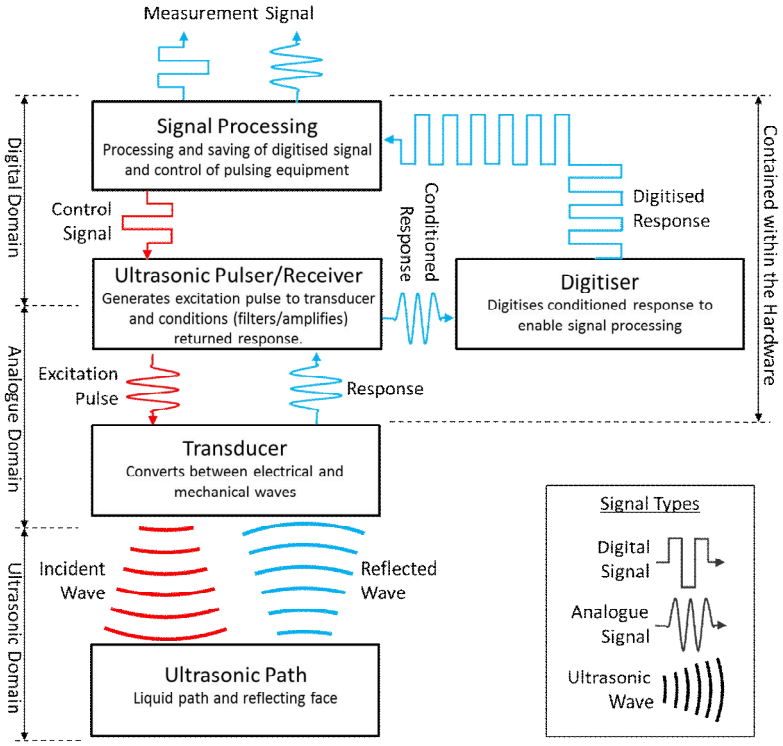

Figure 9: Example Ultrasonic System.

Pulsing/Receiving Hardware
Initial testing was performed using an aeration (vapour bubble) detection unit. This industrialised ultrasonic unit is capable of pulsing at high speed, digitising the returned response and processing this in real time. The output from the device is a 4-20mA signal, which is proportional to the amplitude of the received response.

In signal processing, the Nyquist rate (Chen, 2001) is commonly used as the lower rate for alias-free signal digitising. This stipulates a sampling rate of greater than twice the waveform frequency, however a more commonly used rule of thumb when dealing with pulse based ultrasonic signals is to use a digitising rate at least a factor of ten greater than the wave centre frequency (for the example a minimum of 100MHz digitiser is required for a 10MHz pulse). This enables adequate reconstruction of the signal. In order to match the returned signal amplitude to the digitiser range, the incoming signal is amplified prior to digitisation. Amplification only ensures the best use of the digitiser resolution, reducing quantization error. As it also amplifies any noise, there is no gain in the Signal to Noise Ratio (SNR). Improved signal to noise ratio is achieved by increasing the incident wave amplitude, and by removing sources of Electromagnetic Interference (EMI) through adequate screening of the electronics and cabling.

Transducer
A 10 MHz single element transducer, with an element diameter of 0.236" (6mm), was used during testing. A coupling material was used to couple the ultrasonic source (sensor) to the sink (containment shell). This also removes any air from the interface, introduced due to the microstructure of the two contacting surfaces. This is necessary because the presence of air will cause considerable loss in transmission (as was demonstrated earlier). A gel couplant was used, although other common materials such as liquids, gels, elastomers and permanent bonding (Theobald, n.d.) can also be used depending upon the application.

DETERMINATION OF THE RELATIONSHIP BETWEEN GAS QUANTITY AND OUPUT OF THE ULTRASONIC MONITORING SYSTEM

A test rig was developed to provide a visual representation of gas quantity and to demonstrate the relationship with the milliamp signal response of the ultrasonic vapour monitoring system. The other benefit of this rig was to demonstrate the shape and nature of the gas bubbles. The rig consisted of a clear plastic sampling channel, dimensionally similar to the internal flow channel of an API 685 Frame 2 pump, with the sensor secured to one side and a metallic reflective surface attached to the inside wall of the opposite side of the channel (to reflect the ultrasonic signal back to the sensor for analysis). Compressed nitrogen gas was injected into the channel, so that the quantity could be varied and measured using a rotameter. Liquid was pumped through the channel at a flow rate that was comparative to the flow rate through the internal flow regime of an API 685 Frame 2 pump. Figure 10 presents a sample of the results obtained from the described test.

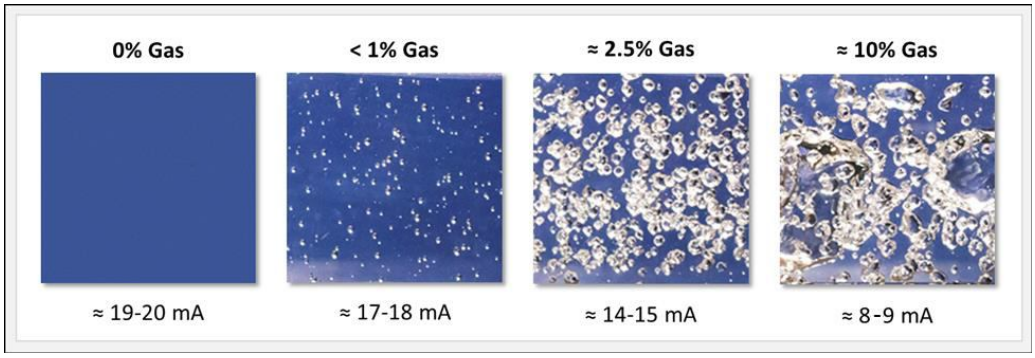

Figure 10: Relationship between Gas Quantity/Bubble Size and the Milliamp Output of the Ultrasonic Vapour Monitoring System.

Without the presence of any gas, the milliamp signal rested between 19 and 20 mA. Less than 1 percent gas was then injected into the sampling channel and the milliamp signal fluctuated between 17 and 18mA. This highlighted the sensitivity of the technology and proved that even the smallest amount of gas has a significant effect on the transmission of the ultrasonic signal through the process liquid in the rear of the pump.

The injection of approximately 10 percent gas produced a range of bubble sizes, including large pockets of gas. This demonstrated that as the quantity of gas increased, the fluctuation of milliamp signal also increased. As expected, a single large bubble passing through the signal path completely blocked the sound wave, which instantly caused the output signal to drop to 4mA. Comparably, a single small bubble caused only a small amount of signal attenuation and the output signal only dropped to 18mA. Thus, the monitoring system was modified to incorporate a complex set of algorithms to counter this and to provide a more accurate representation of the condition within the back of the pump.

APPLICATION OF ULTRASONICS TO PROTECT MAGNETIC-DRIVE PUMPS

Ultrasonic Response to Fault Conditions

A series of extensive tests were carried out in order to determine the response of the ultrasonic vapour monitoring system to a series of fault conditions within a magnetic-drive pump. An API 685 pump was installed in a small test loop (Figure 11), with gate valves on the suction and discharge to control and restrict the flow.

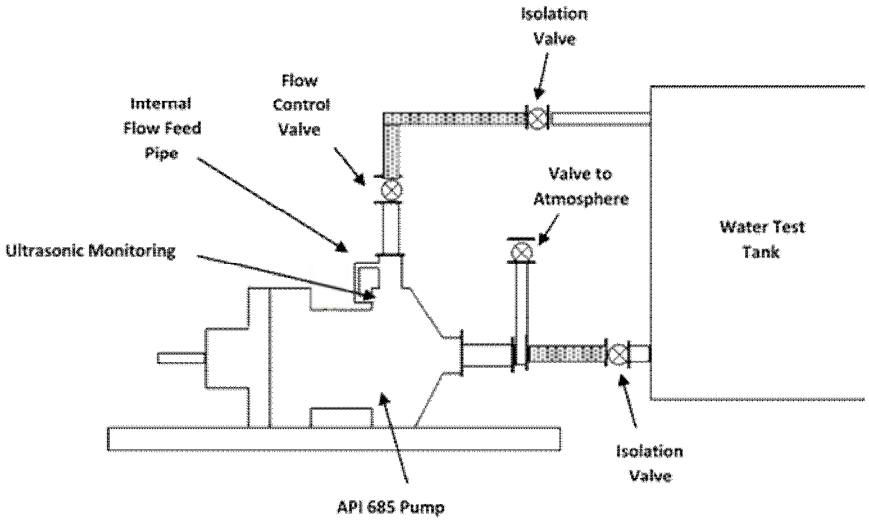

Figure 11: Ultrasonic Vapour Monitoring System Test Loop.

The pump was a 40 bar design and the containment shell was constructed of alloy C276. A reasonably powerful magnetic coupling was selected to ensure that a significant amount of heat was input to the liquid in the internal flow regime due to magnetic coupling losses. The ultrasonic vapour monitoring system was installed through a port in the magnetic coupling housing. This consisted of an ultrasonic sensor, secured to the outside of the containment shell through the port by the means of a clamped olive on a co-axial feedthrough. In addition to the ultrasonic monitoring system, a Resistance Temperature Detector (RTD) probe was installed to measure the temperature of the containment shell.

Liquid Vapourisation in the Internal Flow Regime

A test was performed to replicate vapourisation of liquid in the internal flow regime of a magnetic-drive sealless pump. This condition was induced by performing a closed suction valve test, where the test liquid contained within the pump did not discharge and therefore experienced a temperature rise. Figure 12 presents the response of the ultrasonic monitoring system in relation to the containment shell temperature, when the pump was exposed to suction shut-off condition.

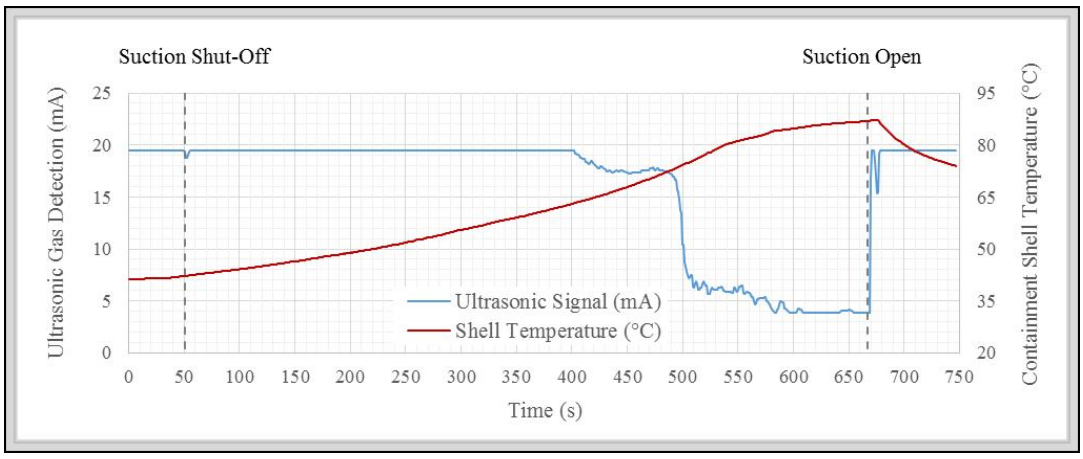

Figure 12: Response of Ultrasonic Vapour Monitoring System to Vapourisation of Liquid in the Internal Flow Regime of Magnetic-Drive. Pump (Blue Trace), with Containment Shell Temperature Overlay (Red Trace).

The pump was run under normal operating conditions until the suction valve was shut at 50 seconds. The temperature of the containment shell immediately began to rise as the fixed volume of liquid was exposed to heating from eddy current losses through the metallic shell. At approximately 400 seconds the ultrasonic monitoring system first began to detect the presence of vapour within the rear of the pump; this was exhibited by the first drop in milliamp signal, caused by increased levels of attenuation of the sound wave and a loss of intensity/amplitude in the signal that returned to the sensor. As the test continued and the containment shell temperature increased further, the milliamp signal briefly 'flattened'; this has been attributed to the transition period between small gas bubbles and larger bubbles forming, comparative to heating a glass container of water and observing entrained gas separating out of solution before the liquid reaches boiling point.

The rapid drop in milliamp signal that occurred after 490 seconds indicates that the liquid began to boil. The temperature of the liquid was very high and combined with the reduction in pressure in the back of the pump, caused by the shut suction valve, meant that larger bubbles began to form. The ultrasonic signal scattered as it encountered the vapour bubbles in the liquid channel, which greatly reduced the intensity/amplitude of the signal that returned to the sensor, presenting as a large drop in milliamp signal. This state was allowed to continue until the liquid in the back of the pump completely vapourised and the milliamp signal dropped to 4 mA. This indicates that the sound wave could not pass through the channel in the back of the pump as it was void of liquid and was instead entirely reflected at the internal boundary of the containment shell.

At 665 seconds, the suction valve was opened and the pump was flooded with cool liquid (at room temperature). The pump recovered almost instantly as the cooler liquid was forced around the internal flow regime and the containment shell temperature began to drop. The ultrasonic monitoring system immediately detected the liquid and the milliamp signal rapidly returned to 19.5 mA as the vapour was forced from the pump. It should be noted that the product lubricated bearings were not damaged during this test. Whilst the liquid was vapourising in the annulus between the inner magnet ring and the containment shell, the bearings remained lubricated.

The significance of these test results is that vapourisation was detected through the use of ultrasonic technology at very early stages, when the liquid was below boiling point. If the milliamp signal was connected to a Distributed Control System (DCS), this would give the user a significant period of time to stop the pump and prevent impending damage.

Gas Slug Entering the Internal Flow Regime

A test was carried out to replicate a slug of gas entering the internal flow regime of the pump. This was achieved by modifying the external pipe that feeds the internal flow regime with liquid, to incorporate a gas injection system (Figure 13).

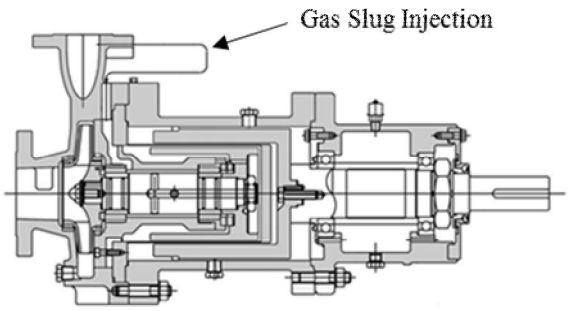

Figure 13: Location of Gas Injection into Magnetic-Drive Pump.

Varying volumes of nitrogen gas were injected into the pump and the response of the ultrasonic monitoring system and shell temperature were recorded (Figure 14).

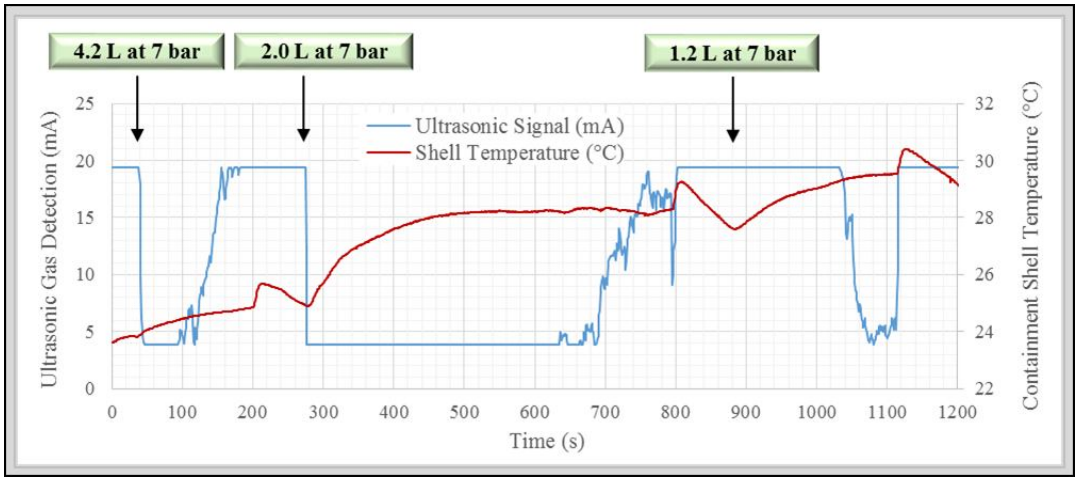

Figure 14: Response of Ultrasonic Vapour Monitoring System to a Gas Slug Entering the Internal Flow Regime of a Magnetic-Drive Pump (Blue Trace), with Containment Shell Temperature Overlay (Red Trace).

As the gas filled the rear of the pump, the temperature of the containment shell increased very quickly as the internal flow regime was completely void of liquid (determined by the ultrasonic monitoring system response to the gas injection). The correlation between shell temperature and the presence of gas in the rear of the pump is significant. The temperature recording validates the milliamp reading, as the shell temperature dropped soon after the gas was forced from the rear of the pump and the milliamp signal returned to 19.5 mA.

A comparison cannot be made between the quantity of gas injected and the length of time that the pump requires to recover from this condition, as it is clear that different quantities of gas will be distributed throughout the pump in very different ways. Despite this, a clear trend has been determined as to the response of the ultrasonic monitoring system.

Ultrasonic Response to Real World Applications

Ultrasonic technology has been applied to monitor the condition of magnetic-drive pumps for a number of different light hydrocarbon services. The following sections present an overview of the experiences of the authors when applying this technology to real world refinery applications.

Intermittent Light Hydrocarbon Application – Horizontal API 685 Pump

A pump user was experiencing operational issues with an existing mechanically sealed API 610 pump when installed on an intermittent light hydrocarbon application. The highly volatile hydrocarbon presented sealing and operational challenges and was causing significant damage to the existing pump; the user had to repair and replace the pump several times, incurring significant cost. A magnetic-drive pump in conformance to API 685 was provided for this application, eliminating the mechanical seal and offering complete containment of the process liquid. The pump was supplied with an engineered composite containment shell, to eliminate the eddy current losses that are associated with metallic containment shells, and ultrasonic vapour monitoring of the internal flow regime to determine any issues with the process or pump operation. This was the first time that ultrasonic monitoring had ever been applied to detect vapour in the internal flow regime of a magnetic-drive pump on a real world application.

The vapour monitoring system was connected to the DCS system and alarm and trip levels were set for the pump based upon the milliamp output. During installation and commissioning of the pump and the ultrasonic vapour monitoring system, an issue was immediately identified. The user followed their standard priming and venting procedure, however it was discovered that the pump was not completely primed when the procedure had reached completion. The ultrasonic sound wave that was received by the sensor was analysed to determine that the internal flow regime was void of liquid. A milliamp signal was generated based upon this reading and was evaluated by the DCS; the pump did not start and damage was prevented. Further investigation showed that the volatile hydrocarbon flashed off immediately as the suction valve was opened to prime the pump. The priming and venting procedure employed by the user did not allow sufficient time for the gaseous hydrocarbon to evacuate the pump and for the hydrocarbon liquid to completely fill the internal flow regime.

The use of this technology assisted the user with forming improved procedures for priming and venting of the pump. This included intricacies such as the percentage that the valves should be opened to when priming and venting, and the maximum time allowable from closure of the vent valve to pump start before the liquid level drops below the sensor and the internal flow regime is void of liquid. This technology is now used approximately three times per day to ensure that the pump is fully primed before operation, preventing potential damage of the pump internals and increasing the reliability of the installation.

Light Hydrocarbon Application – Vertical API 685 Pump

A pump user installed several magnetic-drive vertical pumps in conformance with API 685 to various light hydrocarbon services in an existing facility, as part of an upgrade programme driven by emission issues; all of which were installed with ultrasonic vapour monitoring of the internal flow regime. After successful commissioning and start-up, the user provided some DCS data for analysis and some characteristics/findings are presented in this section.

The operating pressure and liquid vapour pressure were very close for one application and therefore vapourisation was a concern. Upon review of DCS data, the user noted a significant drop in milliamp signal and fluctuation of signal for an extended period of time; the cause of which was unknown. The DCS data from this event is presented in Figure 15.

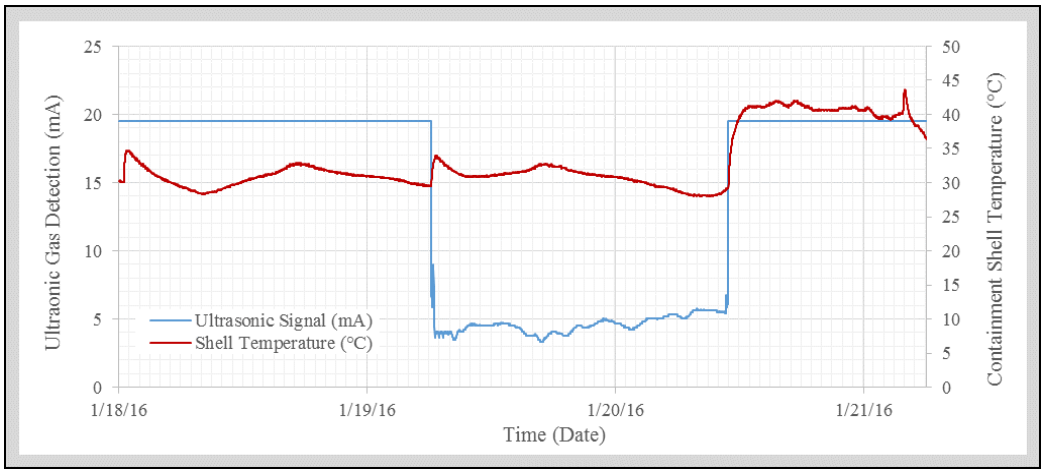

Figure 15: DCS Data from Vertical Pump Applied to Light Hydrocarbon Service, Showing Drop in Ultrasonic Signal (Blue Trace) Plotted Against Containment Shell Temperature (Red Trace).

As described previously (Figure 12), when liquid boils in the rear of an operational pump, the signal will fluctuate at low levels for a very short period of time before settling at 4mA (indicating 100 percent vapour condition). A very different trend was observed here, as the fluctuation at a low milliamp level continued for a period of 24 hours. It was initially determined that the pump was powered down during this event; the sudden recovery in milliamp signal at the end of this period of time indicates that the internal flow regime was flooded with liquid, which can be attributed to either priming the pump or start-up (where the vapour is forced from the internal flow regime). As the signal was fluctuating prior to the milliamp signal recovery, this could not be attributed to pump priming as the signal would have instead shown 4mA (100 percent vapour condition) if the pump was empty; therefore this instant signal recovery could only be caused by start-up of the pump. This is verified by the gradual rise in containment shell temperature as the pump became operational; although it should be noted that the ultrasonic monitoring system detected this change instantaneously, whereas the temperature probe could only be used as verification after a much longer period of time (Figure 16). This is a good demonstration of the responsiveness of ultrasonics to this change in situation, delivering instant feedback to the DCS.

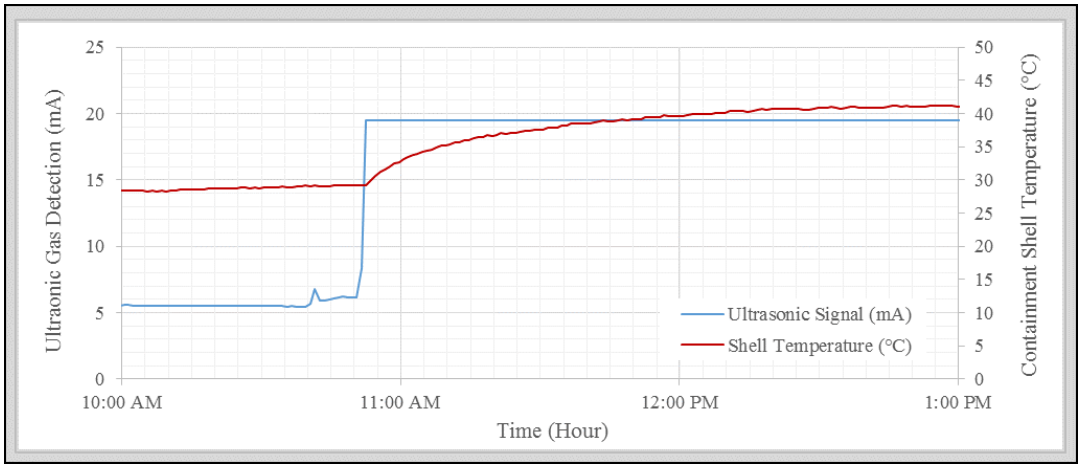

Figure 16: DCS Data from Vertical Pump Applied to Light Hydrocarbon Service, Showing Recover of Ultrasonic Signal (Blue Trace) on Pump Start-Up Compared with Containment Shell Temperature (Red Trace).

When the pump was stopped it is reasonable to assume that it would have been isolated from the process system at the suction and discharge, and therefore an external factor would have caused the initial drop in milliamp signal. The instantaneity of this drop indicates that the liquid experienced a reduction in pressure and vapourised, likely as a result of a purposeful pipe bleed, a leak to atmosphere within the isolated section or a partially open isolation valve.

The low level fluctuation of milliamp signal whilst the pump was not running is as a result of bubble nucleation to the inside wall of the containment shell. Figure 17 presents a visualisation of this condition.

Figure 17: Bubble Nucleation on the Inside Wall of a Containment Shell.

A number of factory tests were carried out to replicate bubble nucleation on the inside wall of the containment shell, to measure the response of the ultrasonic monitoring system. Figure 18 presents the response of the system to this condition, specifically showing the change in amplitude of ultrasonic signal when small gas bubbles form on the shell, in comparison to 100 percent liquid condition.

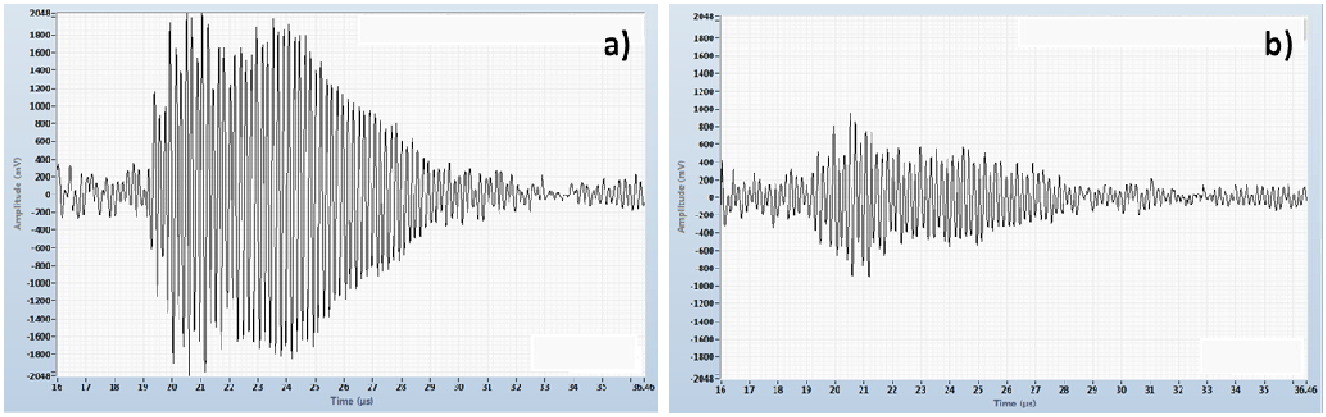

Figure 18: Ultrasonic Reflection from the Pump Bush Holder, Showing the Difference in Signal Amplitude between a) 100 Percent Liquid Condition and b) Bubble Nucleation to the Inside Wall of the Containment Shell.

As can be seen in Figure 18, the amplitude of the ultrasonic signal that is recorded when gas bubbles nucleate to the shell is significantly reduced; however the sound wave does not completely scatter as a reflection a from the bush holder is still defined. The amplitude of the recorded signal is proportional to the milliamp signal output of the unit; the smaller the amplitude, the lower the milliamp signal.

As the sound wave encounters the bubbles on the shell, the majority of the wave will scatter, with a small portion passing through the gaps between the bubbles. Therefore a reduction in milliamp signal will be presented, although complete deterioration of signal will not occur as a portion of the original sound wave will still return to the sensor. The correlation between temperature and ultrasonic signal during the condition presented in Figure 15 should also be considered. The containment shell temperature varied due to the atmospheric conditions on-site, specifically direct sunlight. As the containment shell temperature increased the ultrasonic signal decreased, which indicates that the gas quantity increased and more bubbles formed on the inside wall of the containment shell. Conversely, as the shell temperature decreased the milliamp signal increased.

The detailed analysis and interpretation of the DCS data that has been described herein, could not have been performed by using temperature and thermal monitoring alone. It is clear that ultrasonic technology has provided this user a much greater insight into their magnetic-drive pump processes and operation.

CONCLUSIONS

Ultrasonics can provide advanced and superior monitoring and protection of magnetic-drive centrifugal pumps. Historically, temperature and power measurement devices have been used for pump protection, however these are reactive devices. From ensuring the pump is correctly primed on start-up, to detecting the smallest quantity of entrained vapour separating from solution during the early stages of vapourisation, ultrasonic technology can facilitate a pro-active response to prevent pump damage. Significantly, this is a step forward in the pursuit of improved robustness in magnetic-drive centrifugal pumps.

Whilst the construction of the ultrasonic transmitter (described in this paper) limits its application to only magnetic-drive pumps, the ultrasonic theory behind this technology could be considered for alternative applications. Whilst a solution was found for magnetic-drive pumps, a different application will present different challenges, including installation, process variations and legislation. Therefore the technology would require modification for alternative systems, likely resulting in a range of transducers that are unique to each application. Nevertheless, this technology would certainly benefit a range of applications, resulting in improved equipment security to end user.

NOMENCLATURE

API = American Petroleum Institute
BEP = Best Efficiency Point
DCS = Distributed Control System
EM = Electromagnetic
EMI = Electromagnetic Interference
NDT = Non-Destructive Testing
RTD = Resistance Temperature Detector
SiC = Silicon Carbide
SNR = Signal to Noise Ratio
ToF = Time of Flight
VP = Vapour Pressure

REFERENCES

Alter, K. E., Hallett, M., Karp, B. and Lungu, C., 2012, *Ultrasound-Guided Chemodenervation Procedures: Text and Atlas*, New York: Demos Medical.

API 685, 2011, "Sealless Centrifugal Pumps for Petroleum, Petrochemical, and Gas Industry Process Service," Second Edition, American Petroleum Institute, Washington, DC.

Chen, C. T., 2001, *Digital Signal Processing*, New York: Oxford University Press.

Gaunaurd, G. C. and Überall, H., 1981, "Resonance Theory of Bubbly Liquids," *The Journal of the Acoustical Society of America*, Volume 69, p. 362.

George, D.L., Torczynski, J.R., Shollenberger, K.A., O'Hern, T.J. and Ceccio, S.L., 2000, "Validation of electrical-impedance tomography for measurements of material distribution in two-phase flows," *International Journal of Multiphase Flow*, 26(4), pp. 549-581.

Mason, T. J. and Povey, M. J. W., 1997, *Ultrasound in Food Processing*, London: Blackie Academic & Professional.

Minnaert, M., 1933, "On Musical Air-Bubbles and the Sounds of Running Water," *The London, Edinburgh, and Dublin Philosophical Magazine and Journal of Science*, 16(104), pp. 235-248.

National Physical Laboratory, n.d., Acoustics - The Speed and Attenuation of Sound. [Online] Available at: http://www.kayelaby.npl.co.uk/general_physics/2_4/2_4_1.html [Accessed 15 Feb 2016].

Ozeri, S., Shmilovitz, D. and Fainguelernt, J., 2006, "Ultrasonic Air Bubble Detection Employing Signal Processing Techniques," *2006 IEEE International Symposium on Industrial Electronics*, July, Volume 4, pp. 2840 - 2845.

Povey, M. J. W., 1997, *Ultrasonic Techniques for Fluids Characterization*, San Diego: Academic Press.

Riemer, B.W., Bingham, P.R., Mariam, F.G., Merrill, F.E., 2007, "Measurement of Gas Bubbles in Mercury using Proton Radiography," *Proceedings of 8th International Topical Meeting on Nuclear Applications and Utilization of Accelerators*, pp. 531-537.

Theobald, P., n.d. Guide on Acoustic Emission Sensor Couplants. [Online] Available at: http://www.npl.co.uk/acoustics/ultrasonics/research/guide-on-acoustic-emission-sensor-couplants [Accessed 16 Feb 2016].

Xactex Corporation, n.d. Acoustic Properties for Liquids. [Online] Available at: https://www.nde-

ed.org/GeneralResources/MaterialProperties/UT/ut_matlprop_liquids.htm [Accessed 15 Feb 2016].

Xu, X. and Chahine, G. L., 2010, "Development of an Acoustic Instrument for Bubble Size Distribution Measurement," *Journal of Hydrodynamics*, 22(5), pp. 325-331.

Yim, G. T. and Leighton, T. G., 2010, "Real-Time On-Line Ultrasonic Monitoring for Bubbles in Ceramic 'Slip' in Pottery Pipelines," *Ultrasonics*, 50(1), pp. 60-67.

